

ALICE-PUBLIC-2015-002
13 July 2015

Precision measurement of the mass difference between light nuclei and anti-nuclei with the ALICE experiment at the LHC

ALICE Collaboration*

Abstract

We report on a measurement of the difference $\Delta\mu = \Delta(m/|z|)$ between the mass-over-charge ratio of deuteron (d) and anti-deuteron (\bar{d}), and ${}^3\text{He}$ and ${}^3\bar{\text{He}}$ nuclei, carried out with ALICE (A Large Ion Collider Experiment) in Pb–Pb collisions at a centre-of-mass energy per nucleon pair $\sqrt{s_{\text{NN}}} = 2.76$ TeV. Our measurement yields $\Delta\mu_{\bar{d}d}/\mu_d = [0.9 \pm 0.5(\text{stat.}) \pm 1.4(\text{syst.})] \times 10^{-4}$ and $\Delta\mu_{{}^3\text{He}{}^3\bar{\text{He}}}/\mu_{{}^3\text{He}} = [-1.2 \pm 0.9(\text{stat.}) \pm 1.0(\text{syst.})] \times 10^{-3}$. Combining these results with existing measurements of the masses of the (anti-) nucleons, the relative binding energy differences are extracted, $\Delta\varepsilon_{\bar{d}d}/\varepsilon_d = -0.04 \pm 0.05(\text{stat.}) \pm 0.12(\text{syst.})$ and $\Delta\varepsilon_{{}^3\text{He}{}^3\bar{\text{He}}}/\varepsilon_{{}^3\text{He}} = 0.24 \pm 0.16(\text{stat.}) \pm 0.18(\text{syst.})$. These results test, to an unprecedented precision, the CPT invariance in the sector of light nuclei.

© 2015 CERN for the benefit of the ALICE Collaboration.

Reproduction of this article or parts of it is allowed as specified in the CC-BY-4.0 license.

*See Appendix A for the list of collaboration members

1 Introduction

In ultra relativistic heavy-ion collisions a large amount of energy is deposited in a small volume, allowing for the creation of the Quark Gluon Plasma [1], a phase of matter in which quarks and gluons, normally confined within hadrons, are liberated. After its production, the created system expands and cools down, and the transition into a hadron gas occurs. In the final state of this process a large and similar amount of light nuclei and anti-nuclei is observed [2]. Their yields have been measured at the Relativistic Heavy Ion Collider (RHIC) by the STAR [3] and PHENIX [4] experiments and at the Large Hadron Collider (LHC) by the ALICE [5] experiment. To date, the heaviest anti-nucleus observed [2] is ${}^4\overline{\text{He}}$ (anti- α). For lighter nuclei and anti-nuclei, which are more copiously produced, a detailed comparison of their properties, such as mass and electric charge, is possible. This comparison represents an interesting test of CPT symmetry [6, 7], which implies that all physics laws are the same under the simultaneous reversal of charge(s) (charge conjugation C), reflection of spatial coordinates (parity transformation P) and time inversion (T). Currently, the confirmation of CPT invariance is tested experimentally for elementary fermions [8, 9] and bosons [10], and for Quantum Electrodynamics (QED) [11, 12] and Quantum Chromodynamics (QCD) systems [13–17] (a particular example for the latter being the measurements carried out on neutral kaon decays [18]), with different levels of precision, spanning over several orders of magnitude. The comparison of the mass and the electric charge of a matter particle with the corresponding anti-matter particle, extended from (anti-)baryons to (anti-)nuclei, allows one to probe any difference in the interactions between nucleons and anti-nucleons contributing to the (anti-)nuclei masses. This force is a remnant of the underlying strong interaction among quarks and gluons that can be described by effective theories [19], but not yet directly derived from QCD.

In this note we report the measurements of the difference of the mass-over-charge ratio for deuteron (d) and anti-deuteron (\bar{d}), and for ${}^3\text{He}$ and ${}^3\overline{\text{He}}$ nuclei carried out with the ALICE detector in Pb–Pb collisions at $\sqrt{s_{\text{NN}}} = 2.76$ TeV. These measurements are also used to extract the relative binding energy differences between each nuclear species and its anti-matter counterpart. Section 2 describes the experimental apparatus, the data analysis and the systematic uncertainties. We present the results and the comparison with the published measurements in Section 3. The summary and conclusions are reported in Section 4.

2 Experimental setup and data analysis

The measurements reported in this paper are based on the high-precision tracking and identification capabilities of the ALICE experiment [20] at the LHC. The main detectors used are the ITS [21] (Inner Tracking System), the TPC [22] (Time Projection Chamber), and the TOF [23] (Time Of Flight detector). All three detectors are located inside a solenoidal magnet that produces a magnetic field of 0.5 T directed along the beamline. The ITS, installed around the vacuum beam pipe, has an inner and outer radii of 3.9 cm and 43 cm respectively. It consists of six cylindrical layers: innermost two Silicon Pixel Detectors (SPD), two Silicon Drift Detectors (SDD) in the middle, and outermost two Silicon Strip Detectors (SSD). The ITS is used for track reconstruction of charged particles and provides precise determination of the interaction-vertex position, with resolution better than $20\ \mu\text{m}$ in central Pb–Pb collisions [21]. The TPC surrounds the ITS; it has an inner radius of 85 cm, an external radius of 247 cm and a length along the beam direction close to 500 cm. The TPC has a $90\ \text{m}^3$ drift volume filled with Ne–CO₂ mixture and is divided into two halves by a central membrane, constituting a high-voltage cathode. The TPC end-plates are equipped with Multi-Wire proportional chambers (MWPC). It is the main charged-particle tracking detector of ALICE and provides also the specific energy loss measurement (dE/dx) with a resolution better than 7% in Pb–Pb collisions [20]. The TOF detector is a large-area array of Multigap Resistive Plate Chambers (MRPC), positioned at 370–399 cm from the beam axis and covering the full azimuth and the pseudorapidity range $|\eta| < 0.9$. It provides the measurement of the time of flight (t_{TOF}) of particles with a resolution of 80 ps in Pb–Pb collisions [20].

The analysis is performed using the Pb–Pb data sample collected in 2011, which corresponds to the largest fraction of heavy-ion collisions collected by ALICE so far, at $\sqrt{s_{NN}} = 2.76$ TeV. During the Pb–Pb 2011 run, in order to enrich the selection of central and semi-central collisions¹ and, at the same time, to collect a sample of minimum-bias events for a reference, data were taken using several triggers in parallel. The centrality triggers exploit the amplitude measured by the V0 detectors [25], two scintillator arrays placed around the beam-pipe on either side of the interaction point, covering the pseudorapidity ranges $-3.7 < \eta < -1.7$ and $2.8 < \eta < 5.1$. The minimum-bias trigger requires at least one hit in the SPD and in both V0 detectors. To maximize the number of light (anti-)nuclei available for the analysis, all the physics triggers are accepted and only events tagged as beam–gas interactions [25] are rejected. An additional cut on the distance between the reconstructed primary vertex and the nominal interaction point (10 cm) is used to further reduce the beam-induced background. The final sample consists of about 67 million events. In these events, tracks are selected applying following criteria: a track is required to have at least two associated hits in the ITS (including at least one in the SPD) and at least 70 space points (clusters) in the TPC out of a maximum of 159. The track-fit quality is assured requiring the χ^2 contribution per space point to be less than 4. To exclude the secondary nuclei produced in the detector material, cuts on Distance of Closest Approach of a track to the reconstructed interaction vertex along the beam direction (DCA_z) and in the transverse plane (DCA_{xy}) of 3.2 cm and 0.1 cm, respectively, are used. A stronger cut on DCA_{xy} than on DCA_z was found more effective in reducing contamination from secondaries as discussed below. All tracks that are not matched with a TOF hit are rejected.

Figure 1 shows the TPC dE/dx as a function of rigidity (p/z , where p is the momentum and z the electric charge in units of the elementary charge e) for reconstructed charged-particle tracks, together with the parametrization of the Bethe-Block curves for various particle hypothesis. The main contribution to the background is caused by tracks associated to an incorrect TOF hit. This background is reduced by requiring the track dE/dx to be within two standard deviations from the expectation for a given particle type. The dE/dx standard deviation is determined from the measured dE/dx distribution at the corresponding rigidity. The TPC dE/dx selection strongly suppresses this background for rigidities below $p/|z| < 2.0$ GeV/ c for deuterons and protons (down to 4% and 2%, respectively), and for all rigidities for ${}^3\text{He}$ (down to 1%).

At low rigidity a significant amount of the selected nuclei is created in secondary interactions in the detector material and not in the Pb–Pb interactions. Figure 2 shows the DCA_{xy} distribution in selected rigidity intervals. While the distribution of anti-nuclei is centred around the primary vertex position and almost fully contained within $|DCA_{xy}| < 0.1$ cm, the distribution for nuclei exhibits in addition a nearly flat background due to secondary tracks. Restricting the analysis to the deuterons and ${}^3\text{He}$ nuclei with a rigidity above 1.5 GeV/ c and 1 GeV/ c , respectively, the contamination from secondary nuclei is reduced to a level below 3%.

During the propagation through the detector material, the velocity of charged particles decreases, due to the energy losses. Therefore, the TOF measurement determines the velocity averaged along the trajectory, rather than that at the production vertex. However, the track reconstruction, exploiting the Kalman filter [26], corrects for the energy losses and provides the track rigidity measurement at the interaction vertex. Therefore, the reconstructed rigidity is adjusted to the mean one, by means of a correction calculated via a Monte Carlo simulation based on GEANT3 package [27], where the energy losses are accounted for. The size of these corrections for deuteron and ${}^3\text{He}$ is illustrated in Fig. 3, depicting the ratio of the mean to initial rigidities as a function of the velocity $\beta\gamma = p/mc$ at the interaction vertex, where m denotes the particle mass. The corresponding parameterizations are obtained for (anti-)deuteron and (anti-) ${}^3\text{He}$. The same procedure is also applied for lighter (anti-)particles.

¹ In heavy-ion collisions the centrality is a key parameter in the study of the properties of QCD matter because it is directly related to the initial overlap region of the colliding nuclei. The centrality is usually defined [24] by the event multiplicity which is strongly correlated to the the impact parameter of the two nuclei in the transverse plane to the beam direction.

The combined ITS and TPC tracking information is used to determine the track length (L) extrapolated up to the TOF detector. The squared mass-over-charge ratio is then calculated as

$$\mu_{\text{TOF}}^2 \equiv (m/z)_{\text{TOF}}^2 = (p/z)^2 \left[\left(\frac{t_{\text{TOF}}}{L} \right)^2 - \frac{1}{c^2} \right]. \quad (1)$$

The choice of this variable is motivated by the fact that μ_{TOF}^2 is a linear function of the squared time of flight, thus preserving the Gaussian distribution of the measured quantity. For each of the particle species, the mass is extracted by fitting the mass-squared distributions in narrow $p/|z|$ and η intervals, using Gaussian function with an exponential tail that reflects the time signal distribution of the TOF detector. Examples of the mass-squared distributions for (anti-)protons, (anti-)deuterons and (anti-) ^3He candidates are reported in Fig. 4 in selected rigidity intervals.

Using mass differences, rather than masses themselves, allows to reduce the systematic uncertainties related to tracking, spatial alignment (affecting the measurement of the track momentum and length) and time calibration. Despite that, residual effects are still present, due to imperfections in the detector alignment and the description of the magnetic field, which can lead to position-dependent systematic uncertainties. According to Eq. 1 the μ_{TOF}^2 is calculated using the measurements of three variables: the time of flight (t_{TOF}), the rigidity (p/z), and the track length (L). The systematic uncertainty due to the uncertainty on t_{TOF} is practically eliminated in the mass difference. The dominant contribution to the uncertainty of the mass difference is caused by uncertainty in p/z measurement and its influence on L (the correlated part of the length measurement error) can reach up to 1%. However, these contributions are practically mass independent, therefore they are to the large extent suppressed by rescaling the masses obtained for (anti-)deuteron and (anti-) ^3He with the ratio of PDG-to-measured values of masses [28] for (anti-)proton ($\mu_{p(\bar{p})}^{\text{TOF}}$), i.e.

$$\mu_{A(\bar{A})} = \mu_{A(\bar{A})}^{\text{TOF}} \times \frac{\mu_{p(\bar{p})}^{\text{PDG}}}{\mu_{p(\bar{p})}^{\text{TOF}}}, \quad (2)$$

where $(\bar{A})A$ stays for (anti-)deuteron and (anti-) ^3He . The remaining mass-dependent part and the contribution from uncertainty on the L measurement is expected to be symmetric for positive and negative particles when inverting the magnetic field. To estimate the corresponding systematic effect on the mass-over-charge ratio difference and keep this effect under control, both nuclei and anti-nuclei measurements are performed with similar statistics for two opposite magnetic field configurations and then averaged over the rigidity and rapidity interval. Their half difference is taken as the estimate of this systematic uncertainty.

The uncertainty related to the mean rigidity estimation is conservatively evaluated by removing the corrections shown in Fig. 3. While this contribution is significant for the (anti-) ^3He , it is found negligible, relative to the statistical uncertainty, for the (anti-)deuteron. This can be explained considering that the distortions of the rigidity distributions are more significant for heavier nuclei, due to their higher energy losses. The systematic uncertainty due to the fit procedure of the squared mass-over-charge distributions is evaluated by changing the range and the shape of the background function. TPC dE/dx cuts are varied between one and four standard deviations to probe the sensitivity of the fit results on the residual background. Finally, the tracking quality selection on the distance of closest approach of tracks to the vertex is varied to evaluate the influence of secondary particles on the measurement: a significant effect is found at low rigidity for the deuteron where a higher contamination from secondaries (close to 3%) is present. The impact of all sources of systematic uncertainties is shown in Fig. 5 where the observed maximal deviations are reported. These maximal deviations (Δ) are expressed as standard deviations ($\Delta/\sqrt{12}$, assuming for them a flat probability distribution) and used as the systematic uncertainties that are reported in Table 1.

| Systematic uncertainty | $\Delta\mu_{\text{d}\bar{\text{d}}}/\mu_{\text{d}}$ ($\times 10^{-4}$) | | $\Delta\mu_{{}^3\text{He}^3\bar{\text{He}}}/\mu_{{}^3\text{He}}$ ($\times 10^{-3}$) | |
|--------------------------|---|-----------|--|-----------|
| | 1.5 GeV/c | 4.0 GeV/c | 1.0 GeV/c | 3.0 GeV/c |
| Tracking and alignment | ± 0.7 | | negligible | |
| Mean rigidity correction | negligible | | ± 0.7 | |
| Fit procedure | ± 0.3 | ± 1 | ± 0.5 | |
| TPC dE/dx selection | ± 0.7 | | ± 0.4 | ± 2.5 |
| Secondaries | ± 1 | ± 0.2 | ± 0.1 | |

Table 1: Main systematic uncertainties on $\Delta\mu/\mu$. See text for more details.

3 Results

The mass-over-charge ratio differences between nuclei and anti-nuclei for deuteron and ${}^3\text{He}$ are evaluated as a function of the rigidity of the tracks, and shown in Fig. 6 together with the final result and the one and two standard deviation uncertainty bands. It is computed as weighted average of the measurements obtained in each rigidity interval. Their statistical and uncorrelated systematic uncertainties are used as the weights. The final systematic uncertainty is then the sum in quadrature of the correlated and uncorrelated systematic uncertainties. The measured mass-over-charge ratio differences are

$$\Delta\mu_{\text{d}\bar{\text{d}}} = [1.7 \pm 0.9(\text{stat.}) \pm 2.6(\text{syst.})] \times 10^{-4} \text{ GeV}/c^2, \quad (3)$$

$$\Delta\mu_{{}^3\text{He}^3\bar{\text{He}}} = [-1.7 \pm 1.2(\text{stat.}) \pm 1.4(\text{syst.})] \times 10^{-3} \text{ GeV}/c^2, \quad (4)$$

corresponding to

$$\frac{\Delta\mu_{\text{d}\bar{\text{d}}}}{\mu_{\text{d}}} = [0.9 \pm 0.5(\text{stat.}) \pm 1.4(\text{syst.})] \times 10^{-4}, \quad (5)$$

$$\frac{\Delta\mu_{{}^3\text{He}^3\bar{\text{He}}}}{\mu_{{}^3\text{He}}} = [-1.2 \pm 0.9(\text{stat.}) \pm 1.0(\text{syst.})] \times 10^{-3}, \quad (6)$$

where μ_{d} and $\mu_{{}^3\text{He}}$ are the values recommended by CODATA [29]. The mass-over-charge differences are compatible with zero within the estimated uncertainties, in agreement with CPT invariance expectations. These results (Fig. 7, left) represent the highest precision direct measurements of mass differences in the sector of nuclei and they improve by one to two orders of magnitude analogous results originally obtained more than 40 years ago [30–32]. At 90% confidence level the results correspond to

$$\frac{|\Delta\mu_{\text{d}\bar{\text{d}}}|}{\mu_{\text{d}}} < 2.4 \times 10^{-4} \quad (\text{CL} = 90\%), \quad (7)$$

$$\frac{|\Delta\mu_{{}^3\text{He}^3\bar{\text{He}}}|}{\mu_{{}^3\text{He}}} < 2.1 \times 10^{-3} \quad (\text{CL} = 90\%). \quad (8)$$

The result for the (anti-)deuteron is reported in Fig. 8 (in red), which summarizes the best CPT invariance tests obtained to date for particles, nuclei and atoms [9, 10, 12–14, 28, 33]. These measurements can be used to constrain, for different interactions, the parameters of effective field theories with explicit CPT violating terms to the Standard Model Lagrangian, such as the Standard Model Extension [34] (SME).

Given that $z_{\bar{\text{d}}} = -z_{\text{d}}$ and $z_{{}^3\bar{\text{He}}} = -z_{{}^3\text{He}}$ as for the proton and anti-proton [13, 14], the mass-over-charge differences in Eq. 3 and Eq. 4 and the measurement of the mass differences between proton and anti-proton [13, 14] and between neutron and anti-neutron [15, 16] are used to derive the relative binding

energy differences between the two studied particle species. We obtain

$$\frac{\Delta\epsilon_{d\bar{d}}}{\epsilon_d} = -0.04 \pm 0.05 \text{ (stat.)} \pm 0.12 \text{ (syst.)}, \quad (9)$$

$$\frac{\Delta\epsilon_{{}^3\text{He}^3\bar{\text{He}}}}{\epsilon_{{}^3\text{He}}} = 0.24 \pm 0.16 \text{ (stat.)} \pm 0.18 \text{ (syst.)}, \quad (10)$$

where $\epsilon_A = Zm_p + (A - Z)m_n - m_A$, being m_p and m_n the proton and the neutron mass values recommended by PDG [28] and m_A the mass value of the nucleus with atomic number Z and mass number A , recommended by CODATA [29]. The binding energy is more explicitly connected with possible violations of the CPT symmetry in the (anti-)nucleon interaction than the one connected to the (anti-)nucleon masses, the latter being constrained with a precision of 7×10^{-10} for the proton/anti-proton system [13, 14]. The results improve (Fig. 7, right) by a factor two the constraints on CPT invariance inferred by existing measurements [35, 36] in the (anti-)deuteron system. The binding energy difference is determined for the first time in the case of (anti-) ${}^3\text{He}$, with a relative precision comparable to the one obtained in the (anti-)deuteron system.

4 Conclusions

The production of (anti-)nuclei in relativistic heavy-ion collisions at the LHC represents a unique opportunity to test the CPT invariance of nucleon–nucleon interaction using light nuclei. We have measured the mass-over-charge ratio differences for deuteron and ${}^3\text{He}$, improving by one to two orders of magnitude previous results obtained more than 40 years ago [30–32]. Our results are also expressed in terms of binding energy differences. The value obtained for the (anti-)deuteron improves by a factor two the constraints on CPT invariance inferred by existing measurements [35, 36], while in the case of (anti-) ${}^3\text{He}$ it has been determined for the first time, with a relative precision comparable to the one obtained in the (anti-)deuteron system. Remarkably, these improvements are reached in an experiment not specifically dedicated to test the CPT invariance in nuclear systems.

In the forthcoming years the increase in luminosity and centre-of-mass energy at the LHC will allow one to improve the sensitivity of these measurements, and possibly to extend the study to (anti-) ${}^4\text{He}$. Indeed, the statistics is expected to be about three times larger in the coming data-taking period (Run-II) and up to three orders of magnitude larger in the following one (Run-III), scheduled for 2020. The increase in statistical precision will allow for better TPC dE/dx calibration. The detector alignment will be substantially refined and an improvement in the tracking performance is expected from the completion of the azimuthal coverage of the transition radiation detector of the experiment. Also, the remaining uncertainty on the secondary nuclei contamination should significantly decrease, thanks to the installation of an upgraded ITS [37] for the Run-III period.

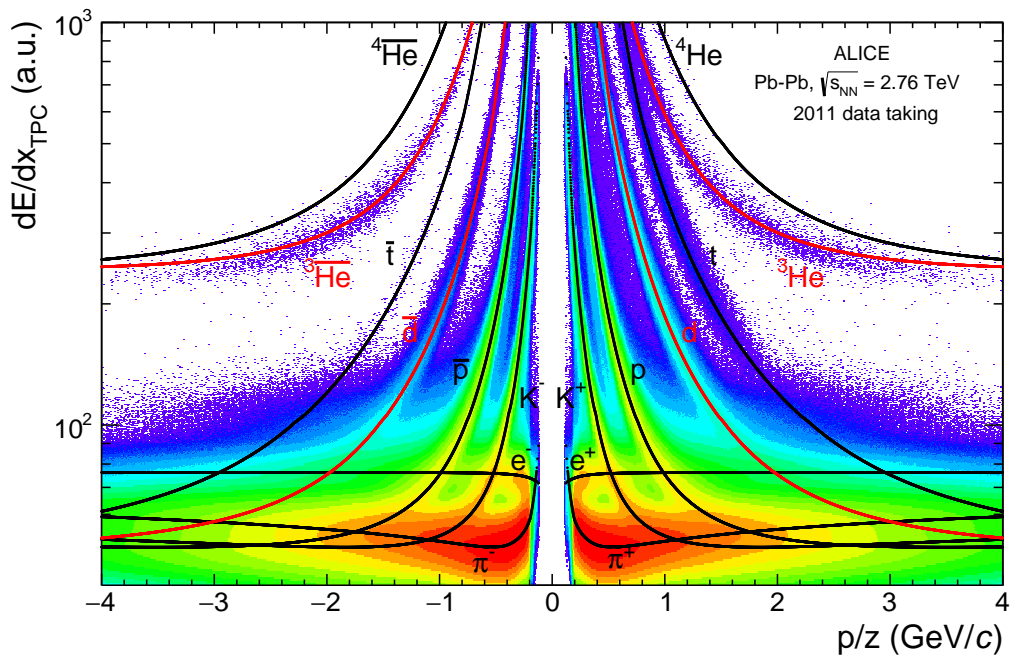


Fig. 1: Specific energy loss of the tracks (dE/dx) in the TPC versus rigidity for negative and positive particles. Lines represent the parameterization of the Bethe-Bloch formula for various particle species (the red lines correspond to (anti-)deuteron and (anti-) ^3He nucleus). Most of the nuclei at low rigidity are produced from the material “knock out”: to reject them, the information of the distance of closest approach of the tracks to the reconstructed primary vertex is used (see text).

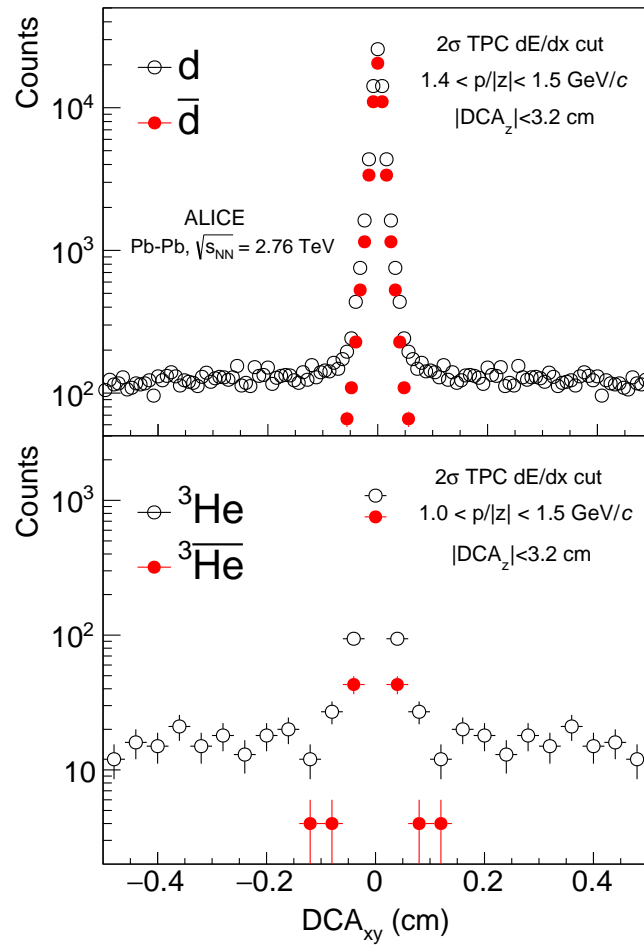


Fig. 2: Distance of Closest Approach of the tracks to the primary vertex in the transverse plane to the beam direction (DCA_{xy}) for deuteron (top) and ${}^3\text{He}$ (bottom). Nuclei and anti-nuclei are shown as empty black points and filled red points, respectively.

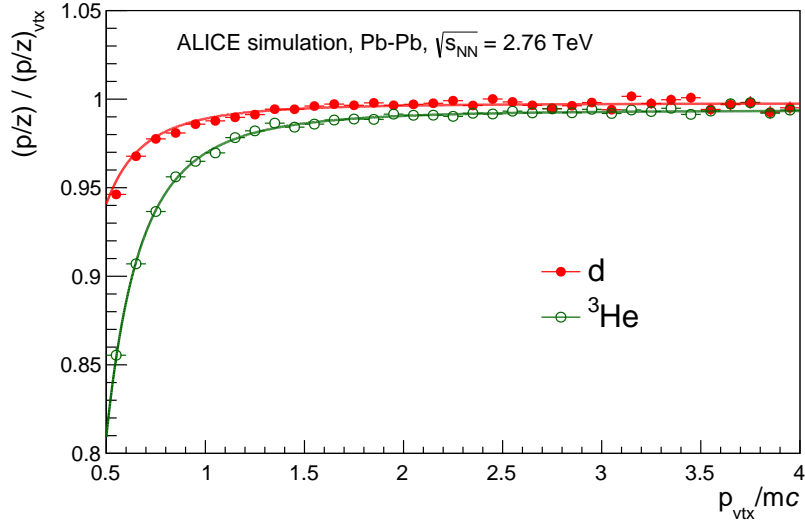


Fig. 3: Ratio between the mean rigidity $\langle p/z \rangle$ and the rigidity at the primary vertex $(p/z)_{\text{vtx}}$ as a function of initial $\beta\gamma = p_{\text{vtx}}/mc$ for deuteron (red filled points) and ${}^3\text{He}$ (green open points) obtained in the Monte Carlo with the detector simulation. The coloured lines indicate the corresponding parameterizations.

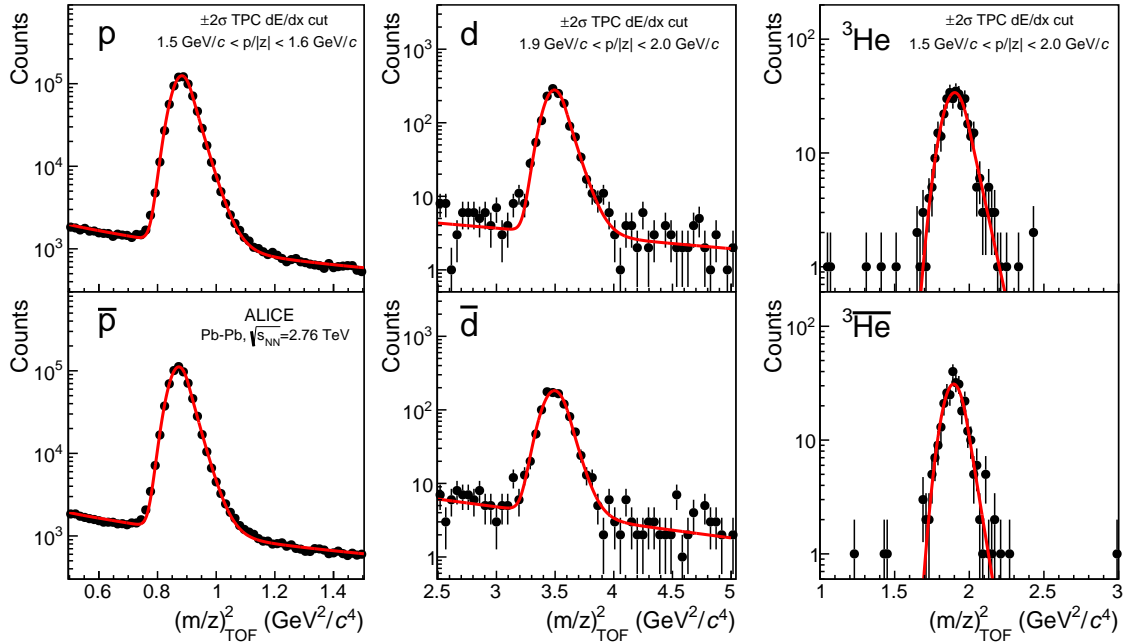


Fig. 4: Examples of squared mass-over-charge ratio distributions for protons (left), deuterons (centre) and ${}^3\text{He}$ (right) in selected rigidity intervals. Particle and anti-particle spectra are in the top and bottom panels, respectively. The fit function (red curve) also includes an exponential term to describe the background. In the rigidity intervals shown here the background corresponds to about 2% for (anti-)protons, and to about 4% for (anti-)deuterons, while it is 0.7% for ${}^3\text{He}$ and ${}^3\bar{\text{He}}$.

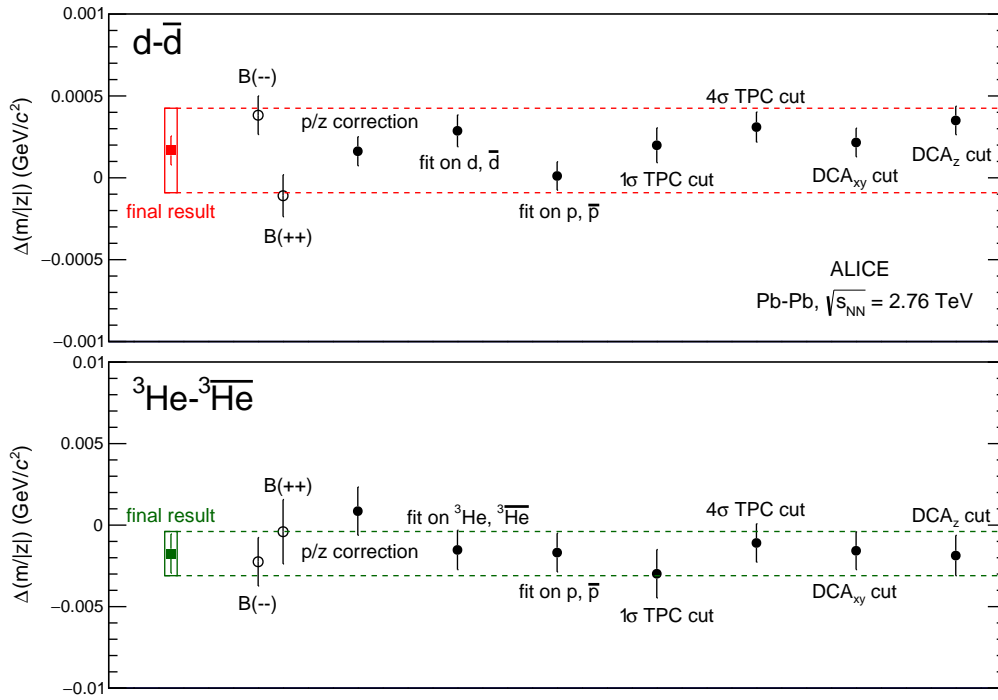


Fig. 5: Distribution of the mass-over-charge ratio difference measurements of $d-\bar{d}$ (top) and ${}^3\text{He}-{}^3\bar{\text{He}}$ (bottom) obtained in the positive and negative magnetic field configurations (black open points labelled as $B(++)$ and $B(+-)$, respectively), by removing the mean rigidity corrections, by varying the fit strategy for (anti-)nuclei and (anti-)protons, the particle selection in the TPC and the requirement on the DCA in the transverse plane and along the beam direction (DCA_{xy} and DCA_z , respectively). These are compared to the final result (red and green squares), shown with its statistical uncertainty (vertical bar) and its systematic uncertainty expressed as standard deviation (open box).

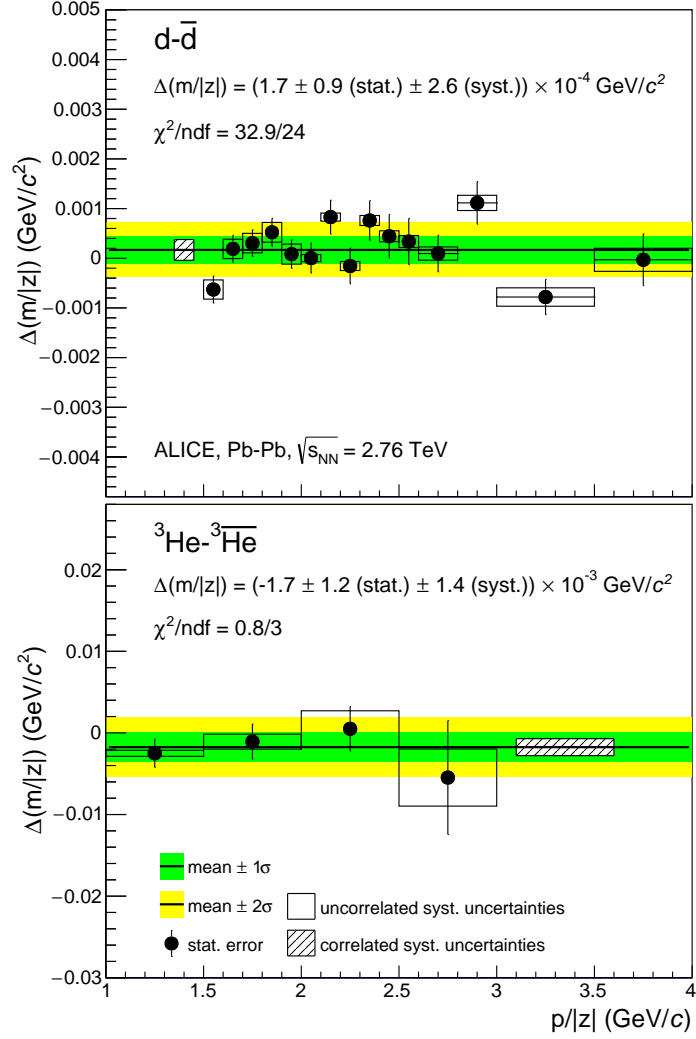


Fig. 6: $d-\bar{d}$ (top) and ${}^3\text{He}-{}^3\overline{\text{He}}$ (bottom) mass-over-charge ratio difference measurements as a function of the particle rigidity. Vertical bars and open boxes show the statistical and the uncorrelated systematic uncertainties, respectively. Both are taken into account to calculate the combined result in the full rigidity range, together with the correlated systematic uncertainty, which is shown as a box with diagonal hatches. Also shown are the 1σ and 2σ bands around the central value, where σ is the sum in quadrature of the statistical and systematic uncertainties.

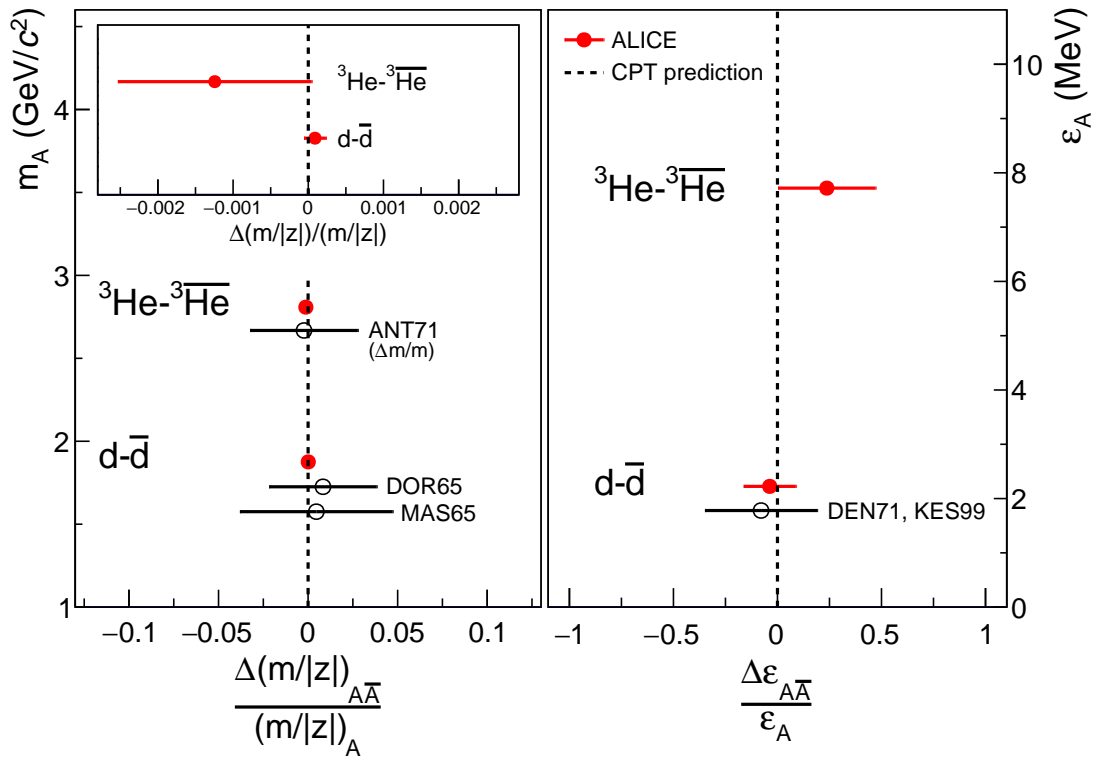


Fig. 7: The ALICE measurements for $d-\bar{d}$ and ${}^3\text{He}-{}^3\bar{\text{He}}$ mass-over-charge ratio differences compared to CPT invariance expectation (dotted lines) and existing mass measurements MAS65 [30], DOR65 [31] and ANT71 [32] (left panel). The inset shows the ALICE results on a finer $\Delta(m/|z|)/(m/|z|)$ scale. The right panel shows our determination of the binding energy differences compared with direct measurements from DEN71 [35] and KES99 [36]. Error bars represent the sum in quadrature of the statistical and systematic uncertainties.

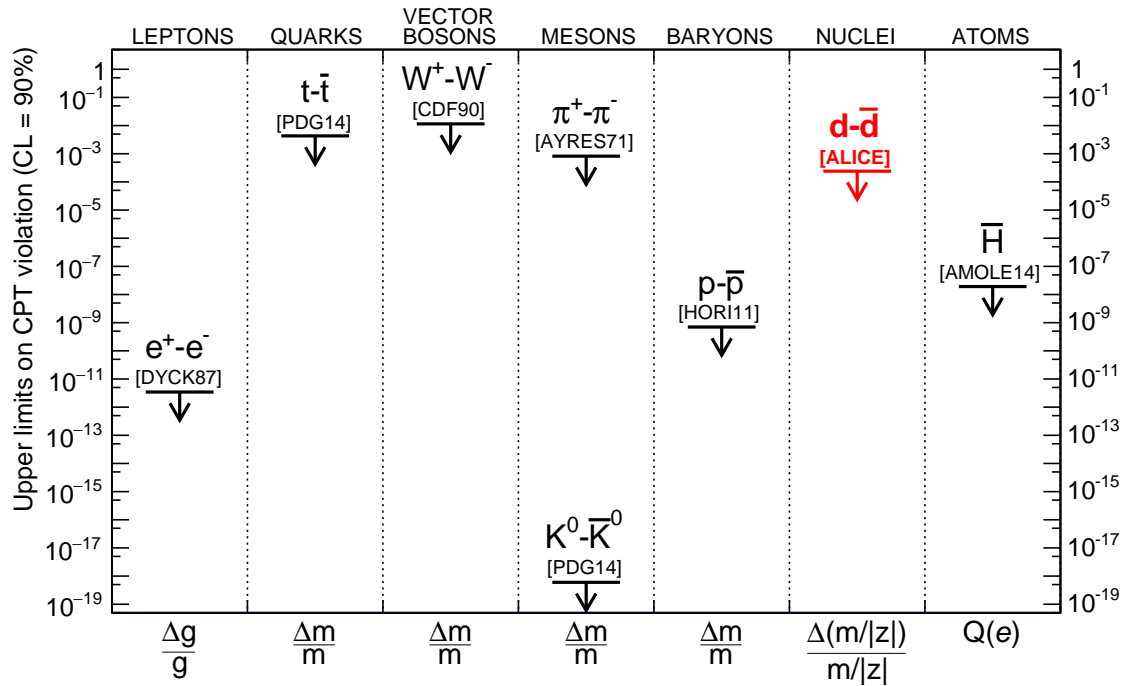


Fig. 8: Experimental limits for CPT invariance (CL = 90%) for particles, nuclei and atoms. From left to right: measurement of g-factor for the electron and positron (DYCK87 [9]), mass difference between top and anti-top (PDG average [28]), $W^+ - W^-$ (CDF90 [10]), $\pi^+ - \pi^-$ (AYRES71 [33]), $K^0 - \bar{K}^0$ (PDG average [28]), proton and anti-proton (HORI11 [13, 14]), deuteron and anti-deuteron (our result) and the charge of anti-hydrogen (AMOLE14 [12]).

References

- [1] P. Braun-Munzinger and J. Stachel, “The quest for the quark-gluon plasma,” *Nature* **448** (2007) 302–309.
- [2] **STAR** Collaboration, H. Agakishiev *et al.*, “Observation of the antimatter helium-4 nucleus,” *Nature* **473** (2011) 353–356, arXiv:1103.3312 [nucl-ex].
- [3] **STAR** Collaboration, J. Harris, “The STAR experiment at the relativistic heavy ion collider,” *Nucl.Phys.* **A566** (1994) 277C–285C.
- [4] **PHENIX** Collaboration, J. Gregory *et al.*, “PHENIX experiment at RHIC,” *Nucl.Phys.* **A566** (1994) 287C–298C.
- [5] **ALICE** Collaboration, K. Aamodt *et al.*, “The ALICE experiment at the CERN LHC,” *JINST* **3** (2008) S08002.
- [6] G. Luders, “On the Equivalence of Invariance under Time Reversal and under Particle-Antiparticle Conjugation for Relativistic Field Theories,” *Kong.Dan.Vid.Sel.Mat.Fys.Med.* **28N5** (1954) 1–17.
- [7] W. Pauli, “Exclusion principle, lorentz group and reflection of space-time and charge,” in *Niels Bohr and the Development of Physics*, P. Wolfgang, ed., pp. 30–51. Pergamon Press, New York, 1955.
- [8] M. Fee, S. Chu, A. Mills, R. Chichester, D. Zuckerman, *et al.*, “Measurement of the positronium $1^3S_1-2^3S_1$ interval by continuous-wave two-photon excitation,” *Phys.Rev.* **A48** (1993) 192–219.
- [9] R. Van Dyck, P. Schwinberg, and H. Dehmelt, “New High Precision Comparison of Electron and Positron g Factors,” *Phys.Rev.Lett.* **59** (1987) 26–29.
- [10] **CDF** Collaboration, F. Abe *et al.*, “A Measurement of the W -boson mass,” *Phys.Rev.Lett.* **65** (1990) 2243–2246.
- [11] **ALPHA** Collaboration, C. Amole *et al.*, “Resonant quantum transitions in trapped antihydrogen atoms,” *Nature* **483** (2012) 439–443.
- [12] **ALPHA** Collaboration, C. Amole *et al.*, “An experimental limit on the charge of antihydrogen,” *Nature Commun.* **5** (2014) 3955.
- [13] **ASACUSA** Collaboration, M. Hori *et al.*, “Two-photon laser spectroscopy of antiprotonic helium and the antiproton-to-electron mass ratio,” *Nature* **475** (2011) 484–488, arXiv:1304.4330 [physics.atom-ph].
- [14] G. Gabrielse, A. Khabbaz, D. Hall, C. Heimann, H. Kalinowsky, *et al.*, “Precision Mass Spectroscopy of the Anti-proton and Proton Using Simultaneously Trapped Particles,” *Phys.Rev.Lett.* **82** (1999) 3198–3201.
- [15] M. Cresti, L. Peruzzo, and G. Sartori, “Measurement Of The Anti-neutron Mass,” *Phys.Lett.* **B177** (1986) 206–210.
- [16] M. Cresti, L. Peruzzo, and G. Sartori, “Errata,” *Phys.Lett.* **B200** (1988) 587–588.
- [17] **ATRAP** Collaboration, J. DiSciaccia *et al.*, “One-Particle Measurement of the Antiproton Magnetic Moment,” *Phys.Rev.Lett.* **110** (2013) 130801, arXiv:1301.6310 [physics.atom-ph].

- [18] **KLOE** Collaboration, F. Ambrosino *et al.*, “Determination of CP and CPT violation parameters in the neutral kaon system using the Bell-Steinberger relation and data from the KLOE experiment,” *JHEP* **0612** (2006) 011, arXiv:hep-ex/0610034 [hep-ex].
- [19] U. van Kolck, “Effective field theory of nuclear forces,” *Prog.Part.Nucl.Phys.* **43** (1999) 337–418, arXiv:nucl-th/9902015 [nucl-th].
- [20] **ALICE** Collaboration, B. B. Abelev *et al.*, “Performance of the ALICE Experiment at the CERN LHC,” *Int.J.Mod.Phys.* **A29** (2014) 1430044, arXiv:1402.4476 [nucl-ex].
- [21] G. Contin, “Performance of the present ALICE Inner Tracking System and studies for the upgrade,” *JINST* **7** (2012) C06007.
- [22] J. Alme, Y. Andres, H. Appelshauser, S. Bablok, N. Bialas, *et al.*, “The ALICE TPC, a large 3-dimensional tracking device with fast readout for ultra-high multiplicity events,” *Nucl.Instrum.Meth.* **A622** (2010) 316–367, arXiv:1001.1950 [physics.ins-det].
- [23] A. Akindinov, A. Alici, A. Agostinelli, P. Antonioli, S. Arce, *et al.*, “Performance of the ALICE Time-Of-Flight detector at the LHC,” *Eur.Phys.J.Plus* **128** (2013) 44.
- [24] **ALICE** Collaboration, B. Abelev *et al.*, “Centrality determination of Pb-Pb collisions at $\sqrt{s_{NN}} = 2.76$ TeV with ALICE,” *Phys.Rev.* **C88** (2013) 044909, arXiv:1301.4361 [nucl-ex].
- [25] **ALICE** Collaboration, E. Abbas *et al.*, “Performance of the ALICE VZERO system,” *JINST* **8** (2013) P10016, arXiv:1306.3130 [nucl-ex].
- [26] R. Fruhwirth, “Application of Kalman filtering to track and vertex fitting,” *Nucl.Instrum.Meth.* **A262** (1987) 444–450.
- [27] R. Brun, F. Carminati, and S. Giani, *GEANT Detector Description and Simulation Tool*. CERN Program Library Long Writeup W5013, Geneva, 1994.
- [28] **Particle Data Group** Collaboration, K. Olive *et al.*, “Review of Particle Physics,” *Chin.Phys.* **C38** (2014) 090001.
- [29] P. J. Mohr, B. N. Taylor, and D. B. Newell, “CODATA Recommended Values of the Fundamental Physical Constants: 2010,” *Rev.Mod.Phys.* **84** (2012) 1527–1605, arXiv:1203.5425 [physics.atom-ph].
- [30] T. Massam, T. Muller, B. Righini, M. Schneegans, and A. Zichichi, “Experimental observation of antideuteron production,” *Nuovo Cim.* **39** (1965) 10–14.
- [31] D. Dorfan, J. Eades, L. Lederman, W. Lee, and C. Ting, “Observation of antideuterons,” *Phys.Rev.Lett.* **14** (1965) 1003–1006.
- [32] Y. Antipov, S. Denisov, S. Donskov, Y. Gorin, V. Kachanov, *et al.*, “Observation of antihelium-3,” *Nucl.Phys.* **B31** (1971) 235–252.
- [33] D. Ayers, A. Cormack, A. Greenberg, R. Kenney, D. Caldwell, *et al.*, “Measurements of the lifetimes of positive and negative pions,” *Phys.Rev.* **D3** (1971) 1051–1063.
- [34] V. A. Kostelecky and N. Russell, “Data Tables for Lorentz and CPT Violation,” *Rev.Mod.Phys.* **83** (2011) 11–31, arXiv:0801.0287 [hep-ph].
- [35] S. Denisov, S. Donskov, Y. Gorin, V. Kachanov, V. Kutjtin, *et al.*, “Measurements of anti-deuteron absorption and stripping cross sections at the momentum 13.3 GeV/c,” *Nucl.Phys.* **B31** (1971) 253–260.

-
- [36] J. Kessler, E.G., “The Deuteron Binding Energy and the Neutron Mass,” *Phys.Lett.* **A255** (1999) 221–229.
- [37] **ALICE** Collaboration, B. Abelev *et al.*, “Technical Design Report for the Upgrade of the ALICE Inner Tracking System,” *J.Phys.* **G41** (2014) 087002.

A The ALICE Collaboration

J. Adam³⁹, D. Adamová⁸², M.M. Aggarwal⁸⁶, G. Aglieri Rinella³⁶, M. Agnello¹¹⁰, N. Agrawal⁴⁷, Z. Ahammed¹³⁰, I. Ahmed¹⁶, S.U. Ahn⁶⁷, I. Aimo^{93,110}, S. Aiola¹³⁵, M. Ajaz¹⁶, A. Akindinov⁵⁷, S.N. Alam¹³⁰, D. Aleksandrov^{99,99}, B. Alessandro¹¹⁰, D. Alexandre¹⁰¹, R. Alfaro Molina⁶³, A. Alici^{104,12}, A. Alkin³, J. Alme³⁷, T. Alt⁴², S. Altinpinar^{18,18}, I. Altsybeev¹²⁹, C. Alves Garcia Prado¹¹⁸, C. Andrei⁷⁷, A. Andronic⁹⁶, V. Anguelov⁹², J. Anielski⁵³, T. Antičić⁹⁷, F. Antinori¹⁰⁷, P. Antonioli¹⁰⁴, L. Aphecetche¹¹², H. Appelshäuser⁵², S. Arcelli²⁸, N. Armesto¹⁷, R. Arnaldi¹¹⁰, T. Aronsson¹³⁵, I.C. Arsene²², M. Arslandok⁵², A. Augustinus³⁶, R. Averbeck⁹⁶, M.D. Azmi^{19,19}, M. Bach⁴², A. Badalà¹⁰⁶, Y.W. Baek⁴³, S. Bagnasco¹¹⁰, R. Bailhache⁵², R. Bala⁸⁹, A. Baldisseri¹⁵, M. Ball⁹¹, F. Baltasar Dos Santos Pedrosa³⁶, R.C. Baral⁶⁰, A.M. Barbano¹¹⁰, R. Barbera²⁹, F. Barile³³, G.G. Barnaföldi¹³⁴, L.S. Barnby¹⁰¹, V. Barret⁶⁹, P. Bartalini⁷, J. Bartke¹¹⁵, E. Bartsch⁵², M. Basile²⁸, N. Bastid⁶⁹, S. Basu¹³⁰, B. Bathen⁵³, G. Batigne¹¹², A. Batista Camejo⁶⁹, B. Batyunya⁶⁵, P.C. Batzing²², I.G. Bearden⁷⁹, H. Beck⁵², C. Bedda¹¹⁰, N.K. Behera^{48,47}, I. Belikov⁵⁴, F. Bellini²⁸, H. Bello Martinez², R. Bellwied¹²⁰, R. Belmont¹³³, E. Belmont-Moreno⁶³, V. Belyaev⁷⁵, G. Bencedi¹³⁴, S. Beole²⁷, I. Berceau⁷⁷, A. Bercuci⁷⁷, Y. Berdnikov⁸⁴, D. Berenyi¹³⁴, R.A. Bertens⁵⁶, D. Berzano^{36,27}, L. Betev³⁶, A. Bhasin⁸⁹, I.R. Bhat⁸⁹, A.K. Bhati⁸⁶, B. Bhattacharjee⁴⁴, J. Bhom¹²⁶, L. Bianchi^{27,120}, N. Bianchi⁷¹, C. Bianchin^{133,56}, J. Bielčik³⁹, J. Bielčiková⁸², A. Bilandžić^{79,79}, S. Biswas^{78,78}, S. Bjelogrić⁵⁶, F. Blanco¹⁰, D. Blau⁹⁹, C. Blume⁵², F. Bock^{73,92}, A. Bogdanov⁷⁵, H. Bøggild⁷⁹, L. Boldizsár¹³⁴, M. Bombara⁴⁰, J. Book⁵², H. Borel¹⁵, A. Borissov⁹⁵, M. Borri⁸¹, F. Bossú⁶⁴, M. Botje⁸⁰, E. Botta²⁷, S. Böttger⁵¹, P. Braun-Munzinger⁹⁶, M. Bregant¹¹⁸, T. Breitner⁵¹, T.A. Broker⁵², T.A. Browning⁹⁴, M. Broz³⁹, E.J. Brucken^{45,45}, E. Bruna¹¹⁰, G.E. Bruno³³, D. Budnikov⁹⁸, H. Buesching⁵², S. Bufalino^{36,110}, P. Buncic³⁶, O. Busch⁹², Z. Buthelezi⁶⁴, J.T. Buxton²⁰, D. Caffarri^{36,30}, X. Cai⁷, H. Caines¹³⁵, L. Calero Diaz⁷¹, A. Caliva⁵⁶, E. Calvo Villar¹⁰², P. Camerini²⁶, F. Carena³⁶, W. Carena³⁶, J. Castillo Castellanos¹⁵, A.J. Castro¹²³, E.A.R. Casula^{25,25}, C. Cavicchioli³⁶, C. Ceballos Sanchez⁹, J. Cepila^{39,39}, P. Cerello¹¹⁰, B. Chang¹²¹, S. Chapeland³⁶, M. Chartier¹²², J.L. Charvet¹⁵, S. Chattopadhyay¹³⁰, S. Chattopadhyay¹⁰⁰, V. Chelnokov³, M. Cherney⁸⁵, C. Cheshkov¹²⁸, B. Cheynis¹²⁸, V. Chibante Barroso³⁶, D.D. Chinellato¹¹⁹, P. Chochula³⁶, K. Choi⁹⁵, M. Chojnacki⁷⁹, S. Choudhury¹³⁰, P. Christakoglou⁸⁰, C.H. Christensen⁷⁹, P. Christiansen³⁴, T. Chujo¹²⁶, S.U. Chung⁹⁵, C. Cicalo¹⁰⁵, L. Cifarelli^{12,28}, F. Cindolo¹⁰⁴, J. Cleymans⁸⁸, F. Colamaria³³, D. Colella³³, A. Collu²⁵, M. Colocci²⁸, G. Conesa Balbastre⁷⁰, Z. Conesa del Valle⁵⁰, M.E. Connors¹³⁵, J.G. Contreras^{39,11}, T.M. Cormier⁸³, Y. Corrales Morales²⁷, I. Cortés Maldonado², P. Cortese³², M.R. Cosentino¹¹⁸, F. Costa³⁶, P. Crochet⁶⁹, R. Cruz Albino¹¹, E. Cuautle⁶², L. Cunqueiro³⁶, T. Dahms⁹¹, A. Dainese¹⁰⁷, A. Danu⁶¹, D. Das¹⁰⁰, I. Das^{100,50}, S. Das⁴, A. Dash¹¹⁹, S. Dash⁴⁷, S. De^{130,118}, A. De Caro^{31,12}, G. de Cataldo¹⁰³, J. de Cuveland⁴², A. De Falco²⁵, D. De Gruttola^{12,31}, N. De Marco¹¹⁰, S. De Pasquale³¹, A. Deisting^{96,92}, A. Deloff⁷⁶, E. Dénes¹³⁴, G. D'Erasmus³³, D. Di Bari³³, A. Di Mauro³⁶, P. Di Nezza⁷¹, M.A. Diaz Corchero¹⁰, T. Dietel⁸⁸, P. Dillenseger⁵², R. Divià³⁶, Ø. Djuvsland¹⁸, A. Dobrin^{56,80}, T. Dobrowolski^{76,i}, D. Domenicis Gimenez¹¹⁸, B. Dönigus⁵², O. Dordic²², A.K. Dubey¹³⁰, A. Dubla⁵⁶, L. Ducroux¹²⁸, P. Dupieux⁶⁹, R.J. Ehlers¹³⁵, D. Elia¹⁰³, H. Engel⁵¹, B. Erazmus^{112,36}, F. Erhardt¹²⁷, D. Eschweiler⁴², B. Espagnon⁵⁰, M. Estienne¹¹², S. Esumi¹²⁶, D. Evans¹⁰¹, S. Evdokimov¹¹¹, G. Eyyubova³⁹, L. Fabbietti⁹¹, D. Fabris¹⁰⁷, J. Faivre⁷⁰, A. Fantoni⁷¹, M. Fasel⁷³, L. Feldkamp⁵³, D. Felea⁶¹, A. Feliciello¹¹⁰, G. Feofilov¹²⁹, J. Ferencei⁸², A. Fernández Téllez², E.G. Ferreira¹⁷, A. Ferretti²⁷, A. Festanti³⁰, J. Figiel¹¹⁵, M.A.S. Figueredo¹²², S. Filchagin⁹⁸, D. Finogeev⁵⁵, F.M. Fionda¹⁰³, E.M. Fiore³³, M.G. Fleck⁹², M. Floris³⁶, S. Foertsch⁶⁴, P. Foka⁹⁶, S. Fokin⁹⁹, E. Fragiaco¹⁰⁹, A. Francescon^{36,30}, U. Frankenfeld⁹⁶, U. Fuchs³⁶, C. Furget⁷⁰, A. Furs⁵⁵, M. Fusco Girard³¹, J.J. Gaardhøje⁷⁹, M. Gagliardi²⁷, A.M. Gago¹⁰², M. Gallio²⁷, D.R. Gangadharan⁷³, P. Ganotti⁸⁷, C. Gao⁷, C. Garabatos⁹⁶, E. Garcia-Solis¹³, C. Gargiulo³⁶, P. Gasik⁹¹, M. Germain¹¹², A. Gheata³⁶, M. Gheata^{61,36}, P. Ghosh¹³⁰, S.K. Ghosh⁴, P. Gianotti⁷¹, P. Giubellino³⁶, P. Giubilato³⁰, E. Gladysz-Dziadus¹¹⁵, P. Glässel⁹², A. Gomez Ramirez⁵¹, P. González-Zamora¹⁰, S. Gorbunov⁴², L. Görlich¹¹⁵, S. Gotovac¹¹⁴, V. Grabski⁶³, L.K. Graczykowski¹³², A. Grelli⁵⁶, A. Grigoras³⁶, C. Grigoras³⁶, V. Grigoriev⁷⁵, A. Grigoryan¹, S. Grigoryan⁶⁵, B. Grinyov³, N. Grion¹⁰⁹, J.F. Grosse-Oetringhaus³⁶, J.-Y. Grossiord¹²⁸, R. Grosso³⁶, F. Guber⁵⁵, R. Guernane⁷⁰, B. Guerzoni²⁸, K. Gulbrandsen⁷⁹, H. Gulkanyan¹, T. Gunji¹²⁵, A. Gupta⁸⁹, R. Gupta⁸⁹, R. Haake⁵³, Ø. Haaland¹⁸, C. Hadjidakis⁵⁰, M. Haiduc⁶¹, H. Hamagaki¹²⁵, G. Hamar¹³⁴, L.D. Hanratty¹⁰¹, A. Hansen⁷⁹, J.W. Harris¹³⁵, H. Hartmann⁴², A. Harton¹³, D. Hatzifotiadou¹⁰⁴, S. Hayashi¹²⁵, S.T. Heckel⁵², M. Heide⁵³, H. Helstrup³⁷, A. Herghelegiu⁷⁷, G. Herrera Corral¹¹, B.A. Hess³⁵, K.F. Hetland³⁷, T.E. Hilden⁴⁵, H. Hillemanns³⁶, B. Hippolyte⁵⁴, P. Hristov³⁶, M. Huang¹⁸, T.J. Humanic²⁰, N. Hussain⁴⁴, T. Hussain¹⁹, D. Hutter⁴², D.S. Hwang²¹, R. Ilkaev⁹⁸, I. Ilkiv⁷⁶, M. Inaba¹²⁶, C. Ionita³⁶, M. Ippolitov^{75,99}, M. Irfan¹⁹, M. Ivanov⁹⁶, V. Ivanov⁸⁴, V. Izucheev¹¹¹, P.M. Jacobs⁷³, C. Jahnke¹¹⁸, H.J. Jang⁶⁷, M.A. Janik¹³², P.H.S.Y. Jayarathna¹²⁰,

C. Jena^{30,30}, S. Jena¹²⁰, R.T. Jimenez Bustamante⁶², P.G. Jones¹⁰¹, H. Jung⁴³, A. Jusko¹⁰¹, P. Kalinak⁵⁸, A. Kalweit³⁶, J. Kamin⁵², J.H. Kang¹³⁶, V. Kaplin⁷⁵, S. Kar¹³⁰, A. Karasu Uysal⁶⁸, O. Karavichev⁵⁵, T. Karavicheva⁵⁵, E. Karpechev⁵⁵, U. Kebschull⁵¹, R. Keidel¹³⁷, D.L.D. Keijdener⁵⁶, M. Keil³⁶, K.H. Khan¹⁶, M.M. Khan¹⁹, P. Khan¹⁰⁰, S.A. Khan¹³⁰, A. Khanzadeev⁸⁴, Y. Kharlov¹¹¹, B. Kileng³⁷, B. Kim¹³⁶, D.W. Kim^{67,43}, D.J. Kim¹²¹, H. Kim¹³⁶, J.S. Kim⁴³, M. Kim⁴³, M. Kim¹³⁶, S. Kim²¹, T. Kim¹³⁶, S. Kirsch⁴², I. Kisel⁴², S. Kiselev⁵⁷, A. Kisiel¹³², G. Kiss¹³⁴, J.L. Klay⁶, C. Klein⁵², J. Klein⁹², C. Klein-Bösing⁵³, A. Kluge³⁶, M.L. Knichel^{92,92}, A.G. Knospe¹¹⁶, T. Kobayashi¹²⁶, C. Kobdaj¹¹³, M. Kofarago³⁶, M.K. Köhler⁹⁶, T. Kollegger^{96,42}, A. Kolojvari¹²⁹, V. Kondratiev¹²⁹, N. Kondratyeva⁷⁵, E. Kondratyuk¹¹¹, A. Konevskikh⁵⁵, C. Kouzinopoulos³⁶, V. Kovalenko¹²⁹, M. Kowalski^{115,36}, S. Kox⁷⁰, G. Koyithatta Meethaleveedu⁴⁷, J. Kral¹²¹, I. Králik⁵⁸, A. Kravčáková⁴⁰, M. Krelina³⁹, M. Kretz⁴², M. Krivda^{101,58}, F. Krizek⁸², E. Kryshen³⁶, M. Krzewicki^{42,96}, A.M. Kubera²⁰, V. Kučera⁸², Y. Kucheriaev^{99,1}, T. Kugathanan³⁶, C. Kuhn⁵⁴, P.G. Kuijer⁸⁰, I. Kulakov⁴², J. Kumar⁴⁷, L. Kumar^{78,86}, P. Kurashvili^{76,76}, A. Kurepin⁵⁵, A.B. Kurepin⁵⁵, A. Kuryakin⁹⁸, S. Kuschpil⁸², M.J. Kweon⁴⁹, Y. Kwon¹³⁶, S.L. La Pointe¹¹⁰, P. La Rocca²⁹, C. Lagana Fernandes¹¹⁸, I. Lakomov^{50,36}, R. Langoy⁴¹, C. Lara⁵¹, A. Lardeux¹⁵, A. Lattuca²⁷, E.audi³⁶, R. Lea²⁶, L. Leardini⁹², G.R. Lee¹⁰¹, S. Lee¹³⁶, I. Legrand³⁶, J. Lehnert⁵², R.C. Lemmon⁸¹, V. Lenti¹⁰³, E. Leogrande⁵⁶, I. León Monzón¹¹⁷, M. Leoncino²⁷, P. Lévai¹³⁴, S. Li^{7,69}, X. Li¹⁴, J. Lien⁴¹, R. Lietava¹⁰¹, S. Lindal²², V. Lindenstruth⁴², C. Lippmann⁹⁶, M.A. Lisa²⁰, H.M. Ljunggren³⁴, D.F. Lodato⁵⁶, P.I. Loenne¹⁸, V.R. Loggins¹³³, V. Loginov⁷⁵, C. Loizides⁷³, X. Lopez⁶⁹, E. López Torres⁹, A. Lowe^{134,134}, X.-G. Lu⁹², P. Luettig⁵², M. Lunardon³⁰, G. Luparello^{26,56}, A. Maevskaya⁵⁵, M. Mager³⁶, S. Mahajan⁸⁹, S.M. Mahmood²², A. Maire⁵⁴, R.D. Majka¹³⁵, M. Malaev⁸⁴, I. Maldonado Cervantes⁶², L. Malinina⁶⁵, D. Mal'Kevich⁵⁷, P. Malzacher⁹⁶, A. Mamonov⁹⁸, L. Manceau¹¹⁰, V. Manko⁹⁹, F. Manso⁶⁹, V. Manzari^{36,103}, M. Marchisone²⁷, J. Mareš⁵⁹, G.V. Margagliotti²⁶, A. Margotti¹⁰⁴, J. Margutti⁵⁶, A. Marín⁹⁶, C. Markert¹¹⁶, M. Marquard⁵², I. Martashvili¹²³, N.A. Martin⁹⁶, J. Martin Blanco¹¹², P. Martinengo³⁶, M.I. Martínez², G. Martínez García¹¹², M. Martinez Pedreira³⁶, Y. Martynov³, A. Mas¹¹⁸, S. Masciocchi⁹⁶, M. Maserà²⁷, A. Masoni¹⁰⁵, L. Massacrier¹¹², A. Mastroserio³³, A. Matyja¹¹⁵, C. Mayer¹¹⁵, J. Mazer¹²³, M.A. Mazzoni¹⁰⁸, D. McDonald¹²⁰, F. Meddi²⁴, A. Menchaca-Rocha⁶³, E. Meninno³¹, J. Mercado Pérez⁹², M. Meres³⁸, Y. Miake¹²⁶, M.M. Mieskolainen⁴⁵, K. Mikhaylov^{57,65}, L. Milano³⁶, J. Milosevic^{22,131}, L.M. Minervini^{103,23}, A. Mischke⁵⁶, A.N. Mishra⁴⁸, D. Miśkowiec⁹⁶, J. Mitra¹³⁰, C.M. Mitu⁶¹, N. Mohammadi⁵⁶, B. Mohanty^{130,78}, L. Molnar⁵⁴, L. Montaño Zetina¹¹, E. Montes¹⁰, M. Morando³⁰, D.A. Moreira De Godoy¹¹², S. Moretto³⁰, A. Morreale¹¹², A. Morsch³⁶, V. Muccifora⁷¹, E. Mudnic¹¹⁴, D. Mühlheim⁵³, S. Muhuri¹³⁰, M. Mukherjee¹³⁰, H. Müller³⁶, J.D. Mulligan¹³⁵, M.G. Munhoz¹¹⁸, S. Murray⁶⁴, L. Musa³⁶, J. Musinsky⁵⁸, B.K. Nandi⁴⁷, R. Nania¹⁰⁴, E. Nappi¹⁰³, M.U. Naru¹⁶, C. Nattrass¹²³, K. Nayak⁷⁸, T.K. Nayak¹³⁰, S. Nazarenko⁹⁸, A. Nedosekin⁵⁷, L. Nellen⁶², F. Ng¹²⁰, M. Nicassio^{96,96}, M. Niculescu^{36,61,61}, J. Niedziela³⁶, B.S. Nielsen⁷⁹, S. Nikolaev⁹⁹, S. Nikulin⁹⁹, V. Nikulin⁸⁴, F. Noferini^{104,12}, P. Nomokonov⁶⁵, G. Nooren⁵⁶, J. Norman¹²², A. Nyman⁹⁹, J. Nystrand¹⁸, H. Oeschler⁹², S. Oh¹³⁵, S.K. Oh⁶⁶, A. Ohlson³⁶, A. Okatan⁶⁸, T. Okubo⁴⁶, L. Olah¹³⁴, J. Oleniacz¹³², A.C. Oliveira Da Silva¹¹⁸, M.H. Oliver¹³⁵, J. Onderwaater⁹⁶, C. Oppedisano¹¹⁰, A. Ortiz Velasquez⁶², A. Oskarsson³⁴, J. Otwinowski^{96,115}, K. Oyama⁹², M. Ozdemir⁵², Y. Pachmayer⁹², P. Pagano³¹, G. Paic⁶², C. Pajares¹⁷, S.K. Pal¹³⁰, J. Pan¹³³, A.K. Pandey⁴⁷, D. Pant⁴⁷, V. Papikyan¹, G.S. Pappalardo¹⁰⁶, P. Pareek⁴⁸, W.J. Park^{96,96}, S. Parmar⁸⁶, A. Passfeld⁵³, V. Paticchio¹⁰³, B. Paul¹⁰⁰, T. Pawlak¹³², T. Peitzmann⁵⁶, H. Pereira Da Costa¹⁵, E. Pereira De Oliveira Filho¹¹⁸, D. Peresunko^{75,99}, C.E. Pérez Lara⁸⁰, V. Peskov^{52,52}, Y. Pestov⁵, V. Petráček³⁹, V. Petrov¹¹¹, M. Petrovici⁷⁷, C. Petta²⁹, S. Piano¹⁰⁹, M. Pikna³⁸, P. Pillot¹¹², O. Pinazza^{104,36}, L. Pinsky¹²⁰, D.B. Piyarathna¹²⁰, M. Płoskoń⁷³, M. Planinic¹²⁷, J. Pluta¹³², S. Pochybova¹³⁴, P.L.M. Podesta-Lerma^{117,117}, M.G. Poghosyan⁸⁵, B. Polichtchouk¹¹¹, N. Poljak¹²⁷, W. Poonsawat¹¹³, A. Pop⁷⁷, S. Porteboeuf-Houssais⁶⁹, J. Porter⁷³, J. Pospisil⁸², S.K. Prasad⁴, R. Preghenella^{104,104,36}, F. Prino¹¹⁰, C.A. Pruneau¹³³, I. Pshenichnov⁵⁵, M. Puccio¹¹⁰, G. Puddu²⁵, P. Pujahari¹³³, V. Punin⁹⁸, J. Putschke¹³³, H. Qvigstad²², A. Rachevski¹⁰⁹, S. Raha⁴, S. Rajput⁸⁹, J. Rak¹²¹, A. Rakotozafindrabe¹⁵, L. Ramello³², R. Raniwala⁹⁰, S. Raniwala⁹⁰, S.S. Räsänen⁴⁵, B.T. Rascanu⁵², D. Rathee⁸⁶, V. Razazi²⁵, K.F. Read¹²³, J.S. Real⁷⁰, K. Redlich⁷⁶, R.J. Reed¹³³, A. Rehman¹⁸, P. Reichelt⁵², M. Reicher⁵⁶, F. Reidt^{92,36}, X. Ren⁷, R. Renfordt⁵², A.R. Reolon⁷¹, A. Reshetin⁵⁵, F. Rettig⁴², J.-P. Revol¹², K. Reygers⁹², V. Riabov⁸⁴, R.A. Ricci⁷², T. Richert³⁴, M. Richter^{22,22}, P. Riedler³⁶, W. Riegler³⁶, F. Riggi²⁹, C. Ristea⁶¹, A. Rivetti¹¹⁰, E. Rocco⁵⁶, M. Rodríguez Cahuanti^{11,2,11}, A. Rodríguez Manso⁸⁰, K. Røed²², E. Rogochaya⁶⁵, D. Rohr⁴², D. Röhrich¹⁸, R. Romita¹²², F. Ronchetti⁷¹, L. Ronflette¹¹², P. Rosnet⁶⁹, A. Rossi³⁶, F. Roukoutakis⁸⁷, A. Roy⁴⁸, C. Roy⁵⁴, P. Roy¹⁰⁰, A.J. Rubio Montero¹⁰, R. Rui²⁶, R. Russo²⁷, E. Ryabinkin⁹⁹, Y. Ryabov⁸⁴, A. Rybicki¹¹⁵, S. Sadovsky¹¹¹, K. Šafařík³⁶, B. Sahlmuller⁵², P. Sahoo⁴⁸, R. Sahoo⁴⁸, S. Sahoo⁶⁰, P.K. Sahu⁶⁰, J. Saini¹³⁰, S. Sakai⁷¹, M.A. Saleh¹³³, C.A. Salgado¹⁷, J. Salzwedel²⁰,

S. Sambyal⁸⁹, V. Samsonov⁸⁴, X. Sanchez Castro⁵⁴, L. Šándor⁵⁸, A. Sandoval⁶³, M. Sano¹²⁶, G. Santagati²⁹, D. Sarkar¹³⁰, E. Scapparone¹⁰⁴, F. Scarlassara³⁰, R.P. Scharenberg⁹⁴, C. Schiaua⁷⁷, R. Schicker⁹², C. Schmidt⁹⁶, H.R. Schmidt³⁵, S. Schuchmann⁵², J. Schukraft³⁶, M. Schulc³⁹, T. Schuster¹³⁵, Y. Schutz^{112,36}, K. Schwarz⁹⁶, K. Schweda⁹⁶, G. Scioli²⁸, E. Scopinich¹¹⁰, R. Scott¹²³, K.S. Seeder¹¹⁸, J.E. Seger⁸⁵, Y. Sekiguchi¹²⁵, I. Selyuzhenkov^{96,96}, K. Senosi⁶⁴, J. Seo^{66,95}, E. Serradilla^{10,63}, A. Sevcenco⁶¹, A. Shabanov⁵⁵, A. Shabetai¹¹², O. Shadura³, R. Shahoyan³⁶, A. Shangaraev¹¹¹, A. Sharma⁸⁹, N. Sharma^{60,123}, K. Shigaki⁴⁶, K. Shtejer^{9,27}, Y. Sibiriak⁹⁹, S. Siddhanta¹⁰⁵, K.M. Sielewicz³⁶, T. Siemiarz⁷⁶, D. Silvermyr^{83,34}, C. Silvestre⁷⁰, G. Simatovic¹²⁷, G. Simonetti³⁶, R. Singaraju¹³⁰, R. Singh^{89,78}, S. Singha^{78,130}, V. Singhal¹³⁰, B.C. Sinha¹³⁰, T. Sinha¹⁰⁰, B. Sitar³⁸, M. Sitta³², T.B. Skaali²², M. Slupecki¹²¹, N. Smirnov¹³⁵, R.J.M. Snellings⁵⁶, T.W. Snellman¹²¹, C. Sogaard³⁴, R. Soltz⁷⁴, J. Song⁹⁵, M. Song¹³⁶, Z. Song⁷, F. Soramel³⁰, S. Sorensen¹²³, M. Spacek³⁹, E. Spiriti⁷¹, I. Sputowska¹¹⁵, M. Spyropoulou-Stassinaki⁸⁷, B.K. Srivastava⁹⁴, J. Stachel⁹², I. Stan⁶¹, G. Stefanek⁷⁶, M. Steinpreis²⁰, E. Stenlund³⁴, G. Steyn⁶⁴, J.H. Stiller⁹², D. Stocco¹¹², P. Strmen³⁸, A.A.P. Suaide¹¹⁸, T. Sugitate⁴⁶, C. Suire⁵⁰, M. Suleymanov¹⁶, R. Sultanov⁵⁷, M. Šumbera⁸², T.J.M. Symons⁷³, A. Szabo³⁸, A. Szanto de Toledo^{118,i}, I. Szarka³⁸, A. Szczepankiewicz³⁶, M. Szymanski¹³², J. Takahashi¹¹⁹, N. Tanaka¹²⁶, M.A. Tangaro³³, J.D. Tapia Takaki^{ii,50}, A. Tarantola Peloni⁵², M. Tariq¹⁹, M.G. Tarzila⁷⁷, A. Tauro³⁶, G. Tejada Muñoz², A. Telesca³⁶, K. Terasaki¹²⁵, C. Terrevoli^{30,25}, B. Teyssier¹²⁸, J. Thäder^{96,73}, D. Thomas^{56,116}, R. Tieulent¹²⁸, A.R. Timmins¹²⁰, A. Toia⁵², S. Trogolo¹¹⁰, V. Trubnikov³, W.H. Trzaska¹²¹, T. Tsuji¹²⁵, A. Tumkin⁹⁸, R. Turrisi¹⁰⁷, T.S. Tveter²², K. Ullaland¹⁸, A. Uras^{128,128}, G.L. Usai²⁵, A. Utrobicic¹²⁷, M. Vajzer⁸², M. Vala⁵⁸, L. Valencia Palomo⁶⁹, S. Vallero²⁷, J. Van Der Maarel⁵⁶, J.W. Van Hoorne³⁶, M. van Leeuwen⁵⁶, T. Vanat⁸², P. Vande Vyvre³⁶, D. Varga¹³⁴, A. Vargas², M. Vargyas¹²¹, R. Varma⁴⁷, M. Vasileiou⁸⁷, A. Vasiliev⁹⁹, A. Vauthier⁷⁰, V. Vechernin¹²⁹, A.M. Veen⁵⁶, M. Veldhoen⁵⁶, A. Velure¹⁸, M. Venaruzzo⁷², E. Vercellin²⁷, S. Vergara Limón², R. Vernet⁸, M. Verweij¹³³, L. Vickovic¹¹⁴, G. Viesti^{30,i}, J. Viinikainen¹²¹, Z. Vilakazi¹²⁴, O. Villalobos Baillie¹⁰¹, A. Vinogradov⁹⁹, L. Vinogradov¹²⁹, Y. Vinogradov⁹⁸, T. Virgili³¹, V. Vislavicius³⁴, Y.P. Viyogi¹³⁰, A. Vodopyanov⁶⁵, M.A. Völk⁹², K. Voloshin⁵⁷, S.A. Voloshin¹³³, G. Volpe^{36,134}, B. von Haller³⁶, I. Vorobyev⁹¹, D. Vranic^{96,36}, J. Vrláková⁴⁰, B. Vulpescu⁶⁹, A. Vyushin⁹⁸, B. Wagner¹⁸, J. Wagner⁹⁶, H. Wang⁵⁶, M. Wang^{7,112}, Y. Wang⁹², D. Watanabe¹²⁶, M. Weber^{36,120}, S.G. Weber⁹⁶, J.P. Wessels⁵³, U. Westerhoff⁵³, J. Wiechula³⁵, J. Wikne²², M. Wilde⁵³, G. Wilk⁷⁶, J. Wilkinson⁹², M.C.S. Williams¹⁰⁴, B. Windelband⁹², M. Winn⁹², C.G. Yaldo¹³³, Y. Yamaguchi¹²⁵, H. Yang^{56,56}, P. Yang⁷, S. Yano⁴⁶, S. Yasnopolskiy⁹⁹, Z. Yin⁷, H. Yokoyama¹²⁶, I.-K. Yoo⁹⁵, V. Yurchenko³, I. Yushmanov⁹⁹, A. Zaborowska¹³², V. Zaccolo⁷⁹, A. Zaman¹⁶, C. Zampolli¹⁰⁴, H.J.C. Zanolli¹¹⁸, S. Zaporozhets⁶⁵, A. Zarochentsev¹²⁹, P. Závada⁵⁹, N. Zaviyalov⁹⁸, H. Zbroszczyk¹³², I.S. Zgura⁶¹, M. Zhalov⁸⁴, H. Zhang⁷, X. Zhang⁷³, Y. Zhang⁷, C. Zhao²², N. Zhigareva⁵⁷, D. Zhou⁷, Y. Zhou⁵⁶, Z. Zhou¹⁸, H. Zhu⁷, J. Zhu^{7,112}, X. Zhu⁷, A. Zichichi^{12,28}, A. Zimmermann⁹², M.B. Zimmermann^{53,36}, G. Zinovjev³, M. Zyzak⁴²

Affiliation notes

ⁱ Deceased

ⁱⁱ Also at: University of Kansas, Lawrence, Kansas, United States

Collaboration Institutes

- ¹ A.I. Alikhanyan National Science Laboratory (Yerevan Physics Institute) Foundation, Yerevan, Armenia
- ² Benemérita Universidad Autónoma de Puebla, Puebla, Mexico
- ³ Bogolyubov Institute for Theoretical Physics, Kiev, Ukraine
- ⁴ Bose Institute, Department of Physics and Centre for Astroparticle Physics and Space Science (CAPSS), Kolkata, India
- ⁵ Budker Institute for Nuclear Physics, Novosibirsk, Russia
- ⁶ California Polytechnic State University, San Luis Obispo, California, United States
- ⁷ Central China Normal University, Wuhan, China
- ⁸ Centre de Calcul de l'IN2P3, Villeurbanne, France
- ⁹ Centro de Aplicaciones Tecnológicas y Desarrollo Nuclear (CEADEN), Havana, Cuba
- ¹⁰ Centro de Investigaciones Energéticas Medioambientales y Tecnológicas (CIEMAT), Madrid, Spain
- ¹¹ Centro de Investigación y de Estudios Avanzados (CINVESTAV), Mexico City and Mérida, Mexico
- ¹² Centro Fermi - Museo Storico della Fisica e Centro Studi e Ricerche "Enrico Fermi", Rome, Italy
- ¹³ Chicago State University, Chicago, Illinois, USA

- 14 China Institute of Atomic Energy, Beijing, China
- 15 Commissariat à l'Énergie Atomique, IRFU, Saclay, France
- 16 COMSATS Institute of Information Technology (CIIT), Islamabad, Pakistan
- 17 Departamento de Física de Partículas and IGFAE, Universidad de Santiago de Compostela, Santiago de Compostela, Spain
- 18 Department of Physics and Technology, University of Bergen, Bergen, Norway
- 19 Department of Physics, Aligarh Muslim University, Aligarh, India
- 20 Department of Physics, Ohio State University, Columbus, Ohio, United States
- 21 Department of Physics, Sejong University, Seoul, South Korea
- 22 Department of Physics, University of Oslo, Oslo, Norway
- 23 Dipartimento di Elettrotecnica ed Elettronica del Politecnico, Bari, Italy
- 24 Dipartimento di Fisica dell'Università 'La Sapienza' and Sezione INFN Rome, Italy
- 25 Dipartimento di Fisica dell'Università and Sezione INFN, Cagliari, Italy
- 26 Dipartimento di Fisica dell'Università and Sezione INFN, Trieste, Italy
- 27 Dipartimento di Fisica dell'Università and Sezione INFN, Turin, Italy
- 28 Dipartimento di Fisica e Astronomia dell'Università and Sezione INFN, Bologna, Italy
- 29 Dipartimento di Fisica e Astronomia dell'Università and Sezione INFN, Catania, Italy
- 30 Dipartimento di Fisica e Astronomia dell'Università and Sezione INFN, Padova, Italy
- 31 Dipartimento di Fisica 'E.R. Caianiello' dell'Università and Gruppo Collegato INFN, Salerno, Italy
- 32 Dipartimento di Scienze e Innovazione Tecnologica dell'Università del Piemonte Orientale and Gruppo Collegato INFN, Alessandria, Italy
- 33 Dipartimento Interateneo di Fisica 'M. Merlin' and Sezione INFN, Bari, Italy
- 34 Division of Experimental High Energy Physics, University of Lund, Lund, Sweden
- 35 Eberhard Karls Universität Tübingen, Tübingen, Germany
- 36 European Organization for Nuclear Research (CERN), Geneva, Switzerland
- 37 Faculty of Engineering, Bergen University College, Bergen, Norway
- 38 Faculty of Mathematics, Physics and Informatics, Comenius University, Bratislava, Slovakia
- 39 Faculty of Nuclear Sciences and Physical Engineering, Czech Technical University in Prague, Prague, Czech Republic
- 40 Faculty of Science, P.J. Šafárik University, Košice, Slovakia
- 41 Faculty of Technology, Buskerud and Vestfold University College, Vestfold, Norway
- 42 Frankfurt Institute for Advanced Studies, Johann Wolfgang Goethe-Universität Frankfurt, Frankfurt, Germany
- 43 Gangneung-Wonju National University, Gangneung, South Korea
- 44 Gauhati University, Department of Physics, Guwahati, India
- 45 Helsinki Institute of Physics (HIP), Helsinki, Finland
- 46 Hiroshima University, Hiroshima, Japan
- 47 Indian Institute of Technology Bombay (IIT), Mumbai, India
- 48 Indian Institute of Technology Indore, Indore (IITI), India
- 49 Inha University, Incheon, South Korea
- 50 Institut de Physique Nucléaire d'Orsay (IPNO), Université Paris-Sud, CNRS-IN2P3, Orsay, France
- 51 Institut für Informatik, Johann Wolfgang Goethe-Universität Frankfurt, Frankfurt, Germany
- 52 Institut für Kernphysik, Johann Wolfgang Goethe-Universität Frankfurt, Frankfurt, Germany
- 53 Institut für Kernphysik, Westfälische Wilhelms-Universität Münster, Münster, Germany
- 54 Institut Pluridisciplinaire Hubert Curien (IPHC), Université de Strasbourg, CNRS-IN2P3, Strasbourg, France
- 55 Institute for Nuclear Research, Academy of Sciences, Moscow, Russia
- 56 Institute for Subatomic Physics of Utrecht University, Utrecht, Netherlands
- 57 Institute for Theoretical and Experimental Physics, Moscow, Russia
- 58 Institute of Experimental Physics, Slovak Academy of Sciences, Košice, Slovakia
- 59 Institute of Physics, Academy of Sciences of the Czech Republic, Prague, Czech Republic
- 60 Institute of Physics, Bhubaneswar, India
- 61 Institute of Space Science (ISS), Bucharest, Romania
- 62 Instituto de Ciencias Nucleares, Universidad Nacional Autónoma de México, Mexico City, Mexico
- 63 Instituto de Física, Universidad Nacional Autónoma de México, Mexico City, Mexico
- 64 iThemba LABS, National Research Foundation, Somerset West, South Africa

- 65 Joint Institute for Nuclear Research (JINR), Dubna, Russia
- 66 Konkuk University, Seoul, South Korea
- 67 Korea Institute of Science and Technology Information, Daejeon, South Korea
- 68 KTO Karatay University, Konya, Turkey
- 69 Laboratoire de Physique Corpusculaire (LPC), Clermont Université, Université Blaise Pascal, CNRS-IN2P3, Clermont-Ferrand, France
- 70 Laboratoire de Physique Subatomique et de Cosmologie, Université Grenoble-Alpes, CNRS-IN2P3, Grenoble, France
- 71 Laboratori Nazionali di Frascati, INFN, Frascati, Italy
- 72 Laboratori Nazionali di Legnaro, INFN, Legnaro, Italy
- 73 Lawrence Berkeley National Laboratory, Berkeley, California, United States
- 74 Lawrence Livermore National Laboratory, Livermore, California, United States
- 75 Moscow Engineering Physics Institute, Moscow, Russia
- 76 National Centre for Nuclear Studies, Warsaw, Poland
- 77 National Institute for Physics and Nuclear Engineering, Bucharest, Romania
- 78 National Institute of Science Education and Research, Bhubaneswar, India
- 79 Niels Bohr Institute, University of Copenhagen, Copenhagen, Denmark
- 80 Nikhef, National Institute for Subatomic Physics, Amsterdam, Netherlands
- 81 Nuclear Physics Group, STFC Daresbury Laboratory, Daresbury, United Kingdom
- 82 Nuclear Physics Institute, Academy of Sciences of the Czech Republic, Řež u Prahy, Czech Republic
- 83 Oak Ridge National Laboratory, Oak Ridge, Tennessee, United States
- 84 Petersburg Nuclear Physics Institute, Gatchina, Russia
- 85 Physics Department, Creighton University, Omaha, Nebraska, United States
- 86 Physics Department, Panjab University, Chandigarh, India
- 87 Physics Department, University of Athens, Athens, Greece
- 88 Physics Department, University of Cape Town, Cape Town, South Africa
- 89 Physics Department, University of Jammu, Jammu, India
- 90 Physics Department, University of Rajasthan, Jaipur, India
- 91 Physik Department, Technische Universität München, Munich, Germany
- 92 Physikalisches Institut, Ruprecht-Karls-Universität Heidelberg, Heidelberg, Germany
- 93 Politecnico di Torino, Turin, Italy
- 94 Purdue University, West Lafayette, Indiana, United States
- 95 Pusan National University, Pusan, South Korea
- 96 Research Division and ExtreMe Matter Institute EMMI, GSI Helmholtzzentrum für Schwerionenforschung, Darmstadt, Germany
- 97 Rudjer Bošković Institute, Zagreb, Croatia
- 98 Russian Federal Nuclear Center (VNIIEF), Sarov, Russia
- 99 Russian Research Centre Kurchatov Institute, Moscow, Russia
- 100 Saha Institute of Nuclear Physics, Kolkata, India
- 101 School of Physics and Astronomy, University of Birmingham, Birmingham, United Kingdom
- 102 Sección Física, Departamento de Ciencias, Pontificia Universidad Católica del Perú, Lima, Peru
- 103 Sezione INFN, Bari, Italy
- 104 Sezione INFN, Bologna, Italy
- 105 Sezione INFN, Cagliari, Italy
- 106 Sezione INFN, Catania, Italy
- 107 Sezione INFN, Padova, Italy
- 108 Sezione INFN, Rome, Italy
- 109 Sezione INFN, Trieste, Italy
- 110 Sezione INFN, Turin, Italy
- 111 SSC IHEP of NRC Kurchatov institute, Protvino, Russia
- 112 SUBATECH, Ecole des Mines de Nantes, Université de Nantes, CNRS-IN2P3, Nantes, France
- 113 Suranaree University of Technology, Nakhon Ratchasima, Thailand
- 114 Technical University of Split FESB, Split, Croatia
- 115 The Henryk Niewodniczanski Institute of Nuclear Physics, Polish Academy of Sciences, Cracow, Poland
- 116 The University of Texas at Austin, Physics Department, Austin, Texas, USA
- 117 Universidad Autónoma de Sinaloa, Culiacán, Mexico

-
- 118 Universidade de São Paulo (USP), São Paulo, Brazil
 - 119 Universidade Estadual de Campinas (UNICAMP), Campinas, Brazil
 - 120 University of Houston, Houston, Texas, United States
 - 121 University of Jyväskylä, Jyväskylä, Finland
 - 122 University of Liverpool, Liverpool, United Kingdom
 - 123 University of Tennessee, Knoxville, Tennessee, United States
 - 124 University of the Witwatersrand, Johannesburg, South Africa
 - 125 University of Tokyo, Tokyo, Japan
 - 126 University of Tsukuba, Tsukuba, Japan
 - 127 University of Zagreb, Zagreb, Croatia
 - 128 Université de Lyon, Université Lyon 1, CNRS/IN2P3, IPN-Lyon, Villeurbanne, France
 - 129 V. Fock Institute for Physics, St. Petersburg State University, St. Petersburg, Russia
 - 130 Variable Energy Cyclotron Centre, Kolkata, India
 - 131 Vinča Institute of Nuclear Sciences, Belgrade, Serbia
 - 132 Warsaw University of Technology, Warsaw, Poland
 - 133 Wayne State University, Detroit, Michigan, United States
 - 134 Wigner Research Centre for Physics, Hungarian Academy of Sciences, Budapest, Hungary
 - 135 Yale University, New Haven, Connecticut, United States
 - 136 Yonsei University, Seoul, South Korea
 - 137 Zentrum für Technologietransfer und Telekommunikation (ZTT), Fachhochschule Worms, Worms, Germany